communications biology

A Nature Portfolio journal

Article

https://doi.org/10.1038/s42003-025-07714-8

Ceruloplasmin administration in the preclinical mouse model of aceruloplasminemia reveals a sex-related variation in biodistribution

Sara Belloli[1,2,6], Cristina Monterisi[1,6], Paolo Rainone[1,2,3], Angela Coliva[1], Alan Zanardi[4], Antonio Conti[4], Andrea Caricasole[5], Rosa Maria Moresco[1,2,3] & Massimo Alessio[4]

Mutations in the ceruloplasmin (CP) gene are responsible for the rare genetic disease aceruloplasminemia characterized by iron accumulation in different organs, including the brain. We previously reported that administration of purified CP in the CP-deficient (*cp*KO) mouse model of the disease, was therapeutically effective. Here we evaluated the bioavailability of the therapeutic protein in different organs of the *cp*KO mouse. The distribution of administered radiolabelled-[^{64}Cu]-CP was assessed in brain and peripheral tissues in vivo and ex vivo. The uptake of [^{64}Cu]-CP in *cp*KO mice varied according to animal sex and age, with a higher accumulation in the cerebellum and liver of males at 6 months of age, while higher levels were observed in the same organs in females at 10 months. Sex-specific variations in the uptake of radiolabelled-CP were genotype-associated, by comparison with wild type mice. Based on these findings, we assessed sex effects on the therapeutic efficacy of the CP-replacement therapy previously performed. Multivariate analysis confirmed that the therapeutic effect was present for both sexes, and this was more pronounced in males than females. Therefore, sex-related variation in CP tissue bioavailability point to the possibility of sex-specific therapeutic regimens in the design of future CP-replacement therapies for aceruloplasminemia.

Ceruloplasmin (CP) is an enzyme that contains multiple copper ions and is primarily produced in the liver, where it is secreted into the bloodstream[1]. Several other cell types produce and secrete CP including the choroid plexus epithelial cells secreting the protein in the cerebrospinal fluid[2–5]. CP serves various functions, with its major role being ferroxidase activity, which holds clinical significance[1,6,7]. As a ferroxidase, CP plays a crucial role in maintaining iron balance by facilitating the release of cellular iron and its incorporation into transferrin for transportation in the bloodstream[1,8–10].

Mutations in the *CP* gene are responsible for aceruloplasminemia (ACP), an extremely rare genetic disorder with adult onset[6,11–13]. Deficiency of CP leads to intracellular iron accumulation and subsequent cellular toxicity, while at the extracellular level it reduces the availability of iron leading to iron-restricted erythropoietic dysfunction and anemia[6,11,13]. Clinically, ACP is characterized by the accumulation of iron in various organs, such as the liver, pancreas, and retina, resulting in liver dysfunction, diabetes, and visual impairment. These symptoms appear years before the onset of severe neurological symptoms caused by progressive neurodegeneration due to iron accumulation in the brain[6,11,13]. In some ACP patients as well as in the CP-deficient mouse model (*cp*KO), there is evidence that the absence of CP contributes to lipid dysmetabolism in both adipose tissue and the liver[3,14–18]. Notably, *cp*KO mice exhibit signs of inflammation in adipose tissue and liver, and present neuroinflammation and neurodegeneration in the brain[3,17–19].

Presently, there is no available treatment for ACP, specifically for addressing the devastating neurological symptoms[6,13]. Management of ACP typically involves iron-chelation therapy, sometimes combined with transfusion of fresh frozen plasma[6,12,20]. However, while iron-chelation therapy effectively reduces systemic iron accumulation, it does not effectively address iron deposition in the brain[21,22]. We reported that an enzyme

[1]Nuclear Medicine and PET Cyclotron Unit, IRCCS-Ospedale San Raffaele, Milano, Italy. [2]Institute of Bioimaging and Complex Biological Systems, CNR, Segrate, MI, Italy. [3]Medicine and Surgery Department, University of Milano – Bicocca, Monza, MB, Italy. [4]Proteome Biochemistry, COSR-Center for Omics Sciences, IRCCS-Ospedale San Raffaele, Milano, Italy. [5]Research and Innovation, Kedrion S.p.A., Loc. Bolognana, Gallicano, LU, Italy. [6]These authors contributed equally: Sara Belloli, Cristina Monterisi. e-mail: alessio.massimo@hsr.it

replacement therapy (ERT) performed with purified, plasma-derived CP in *cp*KO mice resulted in the reduction of neurological symptoms, neuroinflammation and neurodegenerative phenotype[18,19]. Administration of purified CP also has beneficial effects at the systemic level, improving the dysregulation of iron and lipids in the liver and adipose tissue of *cp*KO mice[3,18], and mobilizing accumulated iron from organs which in turn fostered a partial rescue of erythropoiesis[18]. These evidences prompted us to investigate the uptake and biodistribution of therapeutic CP to complement efficacy data with tissue bioavailability information, useful for further development of a CP-replacement therapy. Molecular imaging in ad hoc animal models is a useful step to study the tissue distribution of a radiopharmaceutical which can provide information about disease mechanisms and validate new treatment options in a translational manner. Moreover, positron emission tomography (PET) imaging applied longitudinally[23] could significantly improve the characterization of ACP patients. Thus, we exploited PET imaging which is largely applied for the in vivo monitoring of several dysfunctions as well as for assessing therapy response. For radiolabelling, the ability of CP to bind Copper (Cu) was leveraged by introducing the radioisotope ^{64}Cu in the protein[18]. This radioisotope has a half-life of 12.7 hours and the fate of radiolabeled protein can be followed for a few days when injected in the organism, being also the half-life of circulating CP about 5.5 days in vivo[1]. Therefore, the distribution of ^{64}Cu-CP in male and female *cp*KO mice of 6 and 10 months of age was evaluated, and its concentration in brain and peripheral tissues in vivo and ex vivo was quantified, in comparison with similarly treated wild-type (WT) mice to determine the influence of the genotype on any observed differences. With these data, we assessed the possibility of sex-specific effects in previously reported studies in this ACP mouse model reporting the efficacy of CP-replacement therapy.

Results

Kinetics of [^{64}Cu]-CP-uptake in *cp*KO mice

For the distribution's kinetics analysis *cp*KO animals of six months of age (3 males, 3 females) were injected with [^{64}Cu]-CP and acquired by positron emission tomography/computed tomography (PET/CT) image at three different time points (1, 3 and 21 h) (Fig. 1a). Data from one male was discarded because of an incorrect intravenous injection procedure. Therefore, the [^{64}Cu]-CP kinetics evaluation results of pooled males and females were plotted to identify the optimal time to maximize signal in the tissues of interest ($N = 5$, Fig. 1b). A general decrease of the radiotracer's signal over time was observed after the injection (Fig. 1b). When data were expressed as tissue to background (muscle) ratio (T/B), an increase of radioactivity in bone and liver, a slight increase in cerebrum and a decrease in heart were observed at 21 h (Fig. 1c). Therefore, the 21 h time point was selected to study the existence of sex- or age-specific distribution of [^{64}Cu]-CP.

The uptake and accumulation of administered [^{64}Cu]-CP in *cp*KO mice varies according to animal sex and age

We investigated the biodistribution and accumulation of administered [^{64}Cu]-CP in different organs of the mice during the disease progression in two critical stages: 6 months of age, which corresponds to the presence of systemic symptoms and the onset of neurological symptoms; and at 10 months of age, in which the presence of overt neurodegeneration has been observed[18,19]. The 4 months window between 6 and 10 months of age represents the treatment time window for CP ERT in this mouse model of ACP we previously published[18].

PET/CT analysis in *cp*KO animals at 6 months of age showed a significantly higher [^{64}Cu]-CP uptake in males than females in cerebellum and liver, and a trend towards higher accumulation in the brain stem and heart,

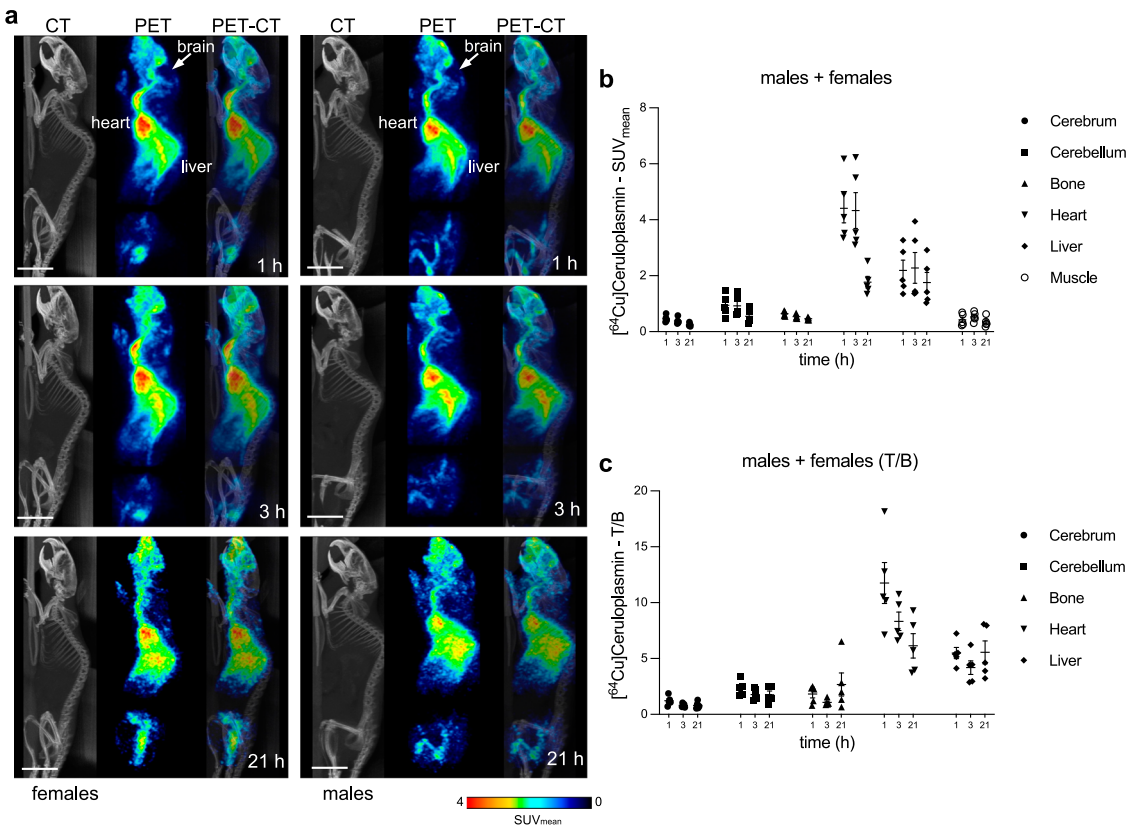

Fig. 1 | Kinetics of [^{64}Cu]-CP-uptake in cpKO mice. a Imaging of [^{64}Cu]-CP radiotracer injected in *cp*KO male and female mice of six months of age for kinetics of distribution determination. A representative image of a female (left) and a male (right) animal are shown for CT, PET and fused modality (from left to right) at the three different time points examined (from top to bottom). Scale bars = 1 cm. **b** PET kinetics in 6 months-old *cp*KO mice after the intravenous injection of [^{64}Cu]-CP ($N = 5$; 3 females + 2 males); radiotracer distribution of males + females expressed as SUV (Mean ± SD). **c** radiotracer distribution of males + females expressed as tissue to background (muscle) (T/B) ratio (Mean ± SD).

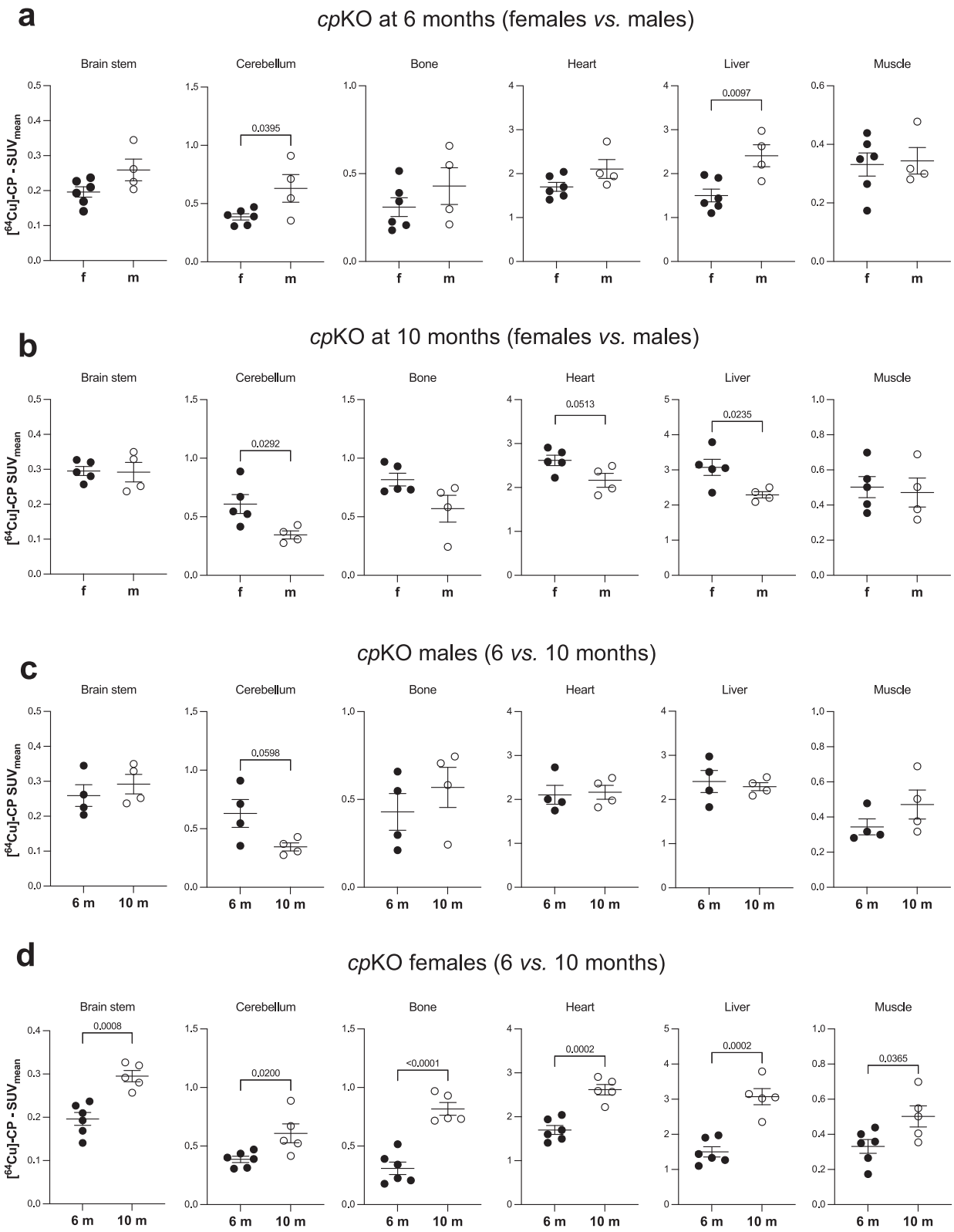

Fig. 2 | In vivo [^{64}Cu]Ceruloplasmin uptake in brain and peripheral tissues of cpKO male and female mice of 6 and 10 months of age. Data are measured at 21 h post injection and are expressed as SUV_{mean} ± SEM, each dot corresponds to one animal (6 months, $N = 6$ females, $N = 4$ males; 10 months, $N = 5$ females, $N = 4$ males). **a**, **b** Comparison of [^{64}Cu]-CP uptake in males vs. females at 6 and 10 months of age, respectively. **c**, **d** Comparison of [^{64}Cu]-CP uptake in 6 vs. 10 months-old male and female mice, respectively. Statistical p-values were evaluated by unpaired Student' *t* test.

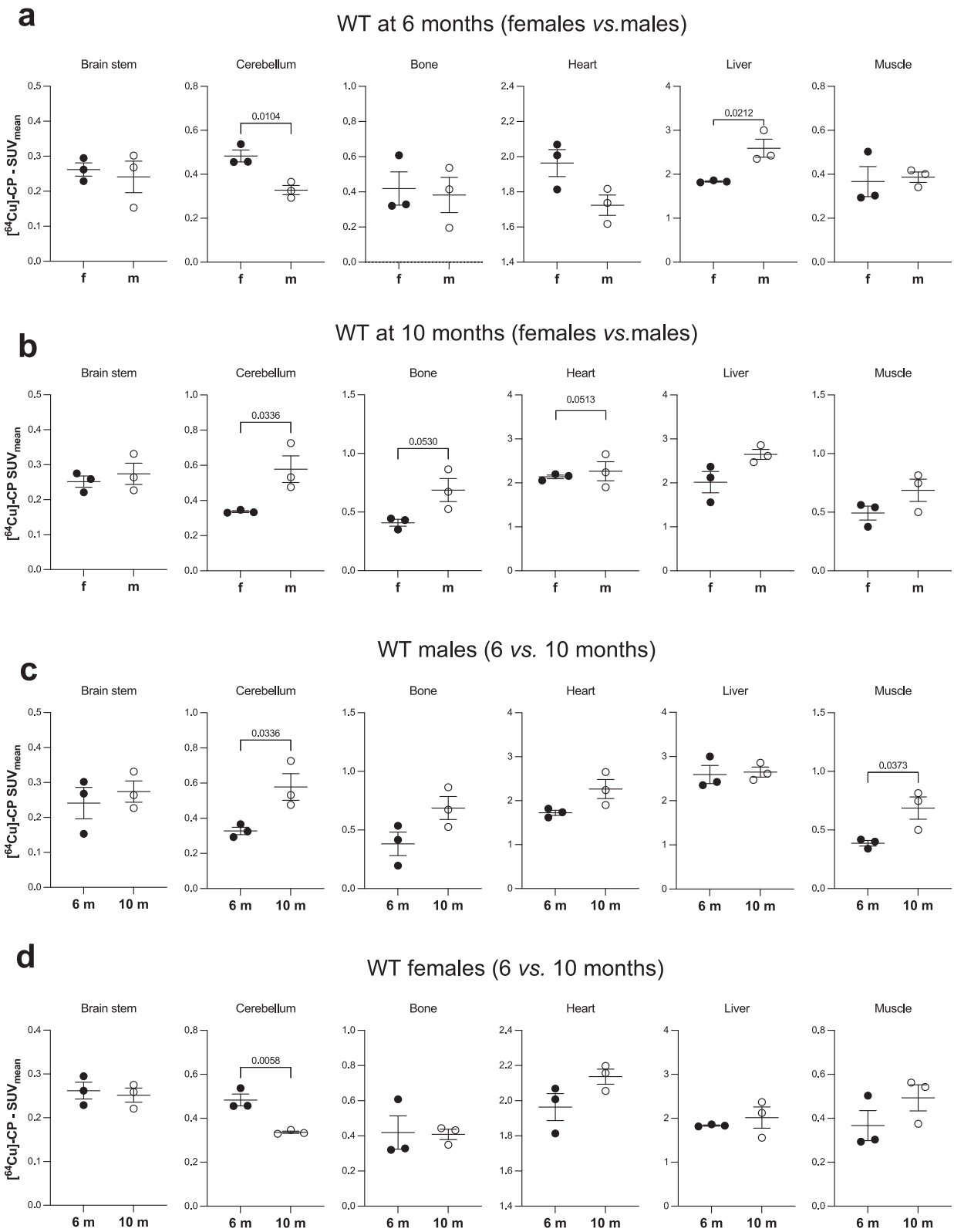

Fig. 3 | In vivo [^{64}Cu]Ceruloplasmin uptake in brain and peripheral tissues of WT male and female mice of 6 and 10 months of age. Data are measured at 21 h post injection and are expressed as SUV_{mean} ± SEM, each dot corresponds to one animal (6 months, $N = 3$ females, $N = 3$ males; 10 months, $N = 3$ females, $N = 3$ males). **a**, **b** Comparison of of [^{64}Cu]-CP uptake in males vs. females at 6 and 10 months of age, respectively. **c**, **d** Comparison of of [^{64}Cu]-CP uptake at 6 vs. 10 months of age in males and females, respectively. Statistical p-values were evaluated by unpaired Student' t-test.

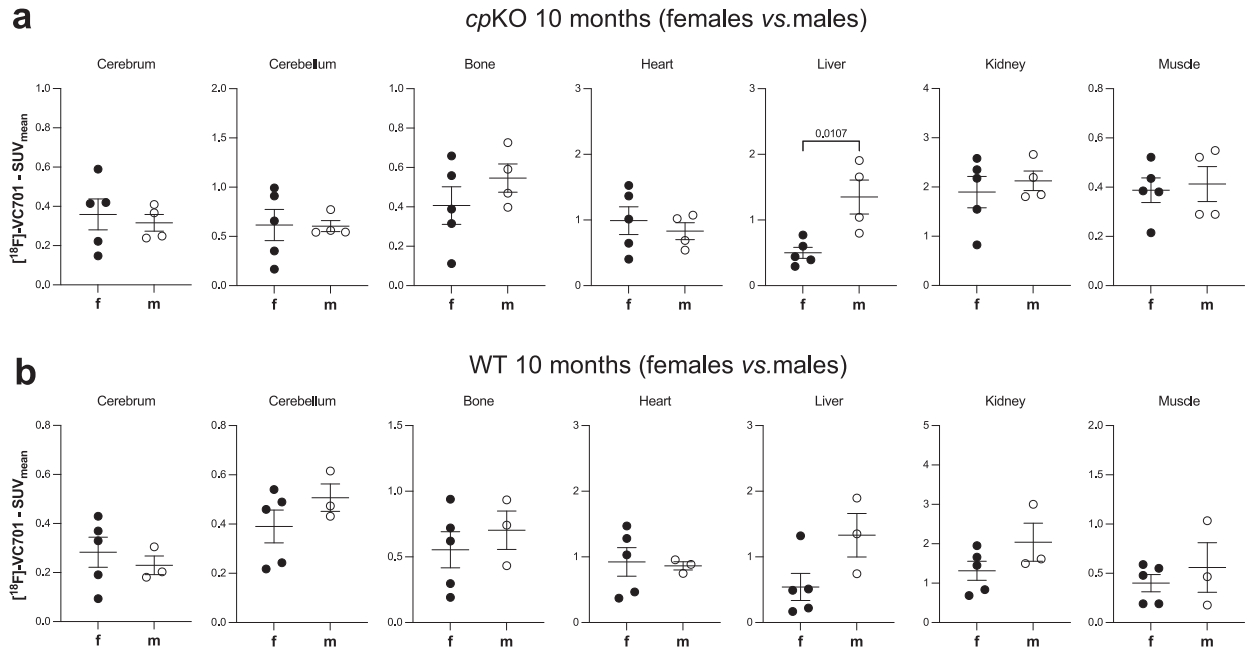

Fig. 4 | In vivo [18F]VC701 uptake in brain and peripheral tissues. a cpKO and **b** WT males and female mice of 10 months of age. Data are measured at 100 min post injection and are expressed as SUV_{mean} ± SEM, each dot corresponds to one animal (*cp*KO, $N = 5$ females, $N = 4$ males; WT, $N = 5$ females, $N = 3$ males). Statistical p-values were evaluated by unpaired Student' t-test.

while similar uptake was observed in bone and muscle (Fig. 2a). Thus, an apparently generalized higher [^{64}Cu]-CP uptake in males than females was observed. Ex vivo biodistribution analysis confirmed a trend for higher [^{64}Cu]-CP uptake in 6 months-old *cp*KO male mice compared to females, which was significant in the brain stem and liver (Supplementary Fig. 1a).

Interestingly, in mice at 10 months of age the PET/CT analysis showed opposite sex-specific effects, i.e. a more robust [^{64}Cu]-CP uptake was observed in *cp*KO female mice rather than in male animals, which was statistically significant in the cerebellum, heart and liver (Fig. 2b). This trend was confirmed also in this case by the ex vivo analysis, in which we observed that the [^{64}Cu]-CP uptake was generally higher in females than males and was significant in liver and muscle (Supplementary Fig. 1b).

Since PET/CT detects radiolabelled Cu, to validate that the signal that we were measuring was a real proxy of the CP protein distribution, as proof of concept we measured by ELISA the CP concentration in the brain lysate of the *cp*KO mice injected with [^{64}Cu]-CP. The results clearly showed that after 21 h from the administration the [^{64}Cu]-CP protein is present in the brain of the mice both at 6 and 10 months of age. (Supplementary Fig. 2).

Analysing the behavior of the [^{64}Cu]-CP uptake in males and females longitudinally in vivo by PET/CT, we observed that the *cp*KO male mice showed equal uptake of [^{64}Cu]-CP in all the organs at 6 and 10 months of age except for cerebellum which showed a near-significant trend of reduction ($p = 0.0598$) of CP uptake in animals at 10 months (Fig. 2c). On the contrary, female mice showed significant increase of [^{64}Cu]-CP uptake in all organs between 6 and 10 months (Fig. 2d). These results indicated a difference in the uptake and accumulation of administered CP in *cp*KO mice which was associated with animal sex and age, showing a higher uptake in males at 6 months of age and vice versa a greater uptake in females at 10 months of age.

Different CP uptake between females and males is sex- and genotype-dependent

To evaluate whether the difference in [^{64}Cu]-CP was a feature associated to sex and age of the mice, independent of an influence of the *cp*KO genotype, we performed the same experiments in WT mice. Similar to the behavior observed in *cp*KO mice, at 6 months of age WT male mice showed significant higher uptake of [^{64}Cu]-CP than females in the liver but showed significant lower uptake in the cerebellum, which is the opposite of the uptake observed in *cp*KO mice (compare Figs. 2a and 3a). At 10 months of age, the opposite [^{64}Cu]-CP uptake to that observed in *cp*KO mice was observed in cerebellum, bone, heart and liver of WT mice, where the uptake was significantly greater in males than females (compare Figs. 2b and 3b). Longitudinally, no significant age-specific differences were observed for both sexes between 6 and 10 months of age, except for the uptake in the cerebellum which did produce an age-specific difference, of an opposite trend to that observed in *cp*KO mice (Fig. 3c, d compared to Fig. 2c, d). Notably, the age-dependent difference between WT and *cp*KO females, with a higher uptake from 6 to 10 months in all organs being observed in *cp*KO mice but not in WT mice (compare Figs. 2d and 3d). Collectively the data indicate that the sex-specific differences in CP uptake observed at different ages in *cp*KO mice is genotype and/or pathology associated.

Higher ^{64}Cu-CP uptake in the liver of *cp*KO females than males at 10 months of age is not dependent on liver inflammation

Since it has been reported that specific differences in the liver uptake of tracers may depend on hepatic inflammatory conditions[23], a study was performed in a satellite group of 10 months-old WT and *cp*KO mice to measure the uptake of the radiotracer [^{18}F]-VC701, a compound reported to specifically target activated macrophages and microglial cells through the binding to the Translocator Protein (TSPO) specific marker[24]. [^{18}F]-VC701 biodistribution measured in vivo with PET/CT showed a significantly higher accumulation of the macrophage specific radiotracer in the liver of *cp*KO males compared to female mice (Fig. 4a). This difference in TSPO marker levels between *cp*KO males and females was significant also by ex vivo sampling (Supplementary Fig. 3). In WT animals no significant sex-related differences in [^{18}F]-VC701 uptake were observed in different organs, even if a trend towards higher [^{18}F]-VC701 uptake was found in the liver of male WT mice (Fig. 4b). The higher uptake of [^{18}F]-VC701 tracer in the liver of WT male mice resulted to be significant in the ex vivo analysis (Supplementary Fig. 3).

To further investigate the different hepatic inflammatory status in male and female *cp*KO mice at both 6 and 10 months of age, macrophage infiltration and Kupffer cell enlargement was evaluated as a proxy for tissue

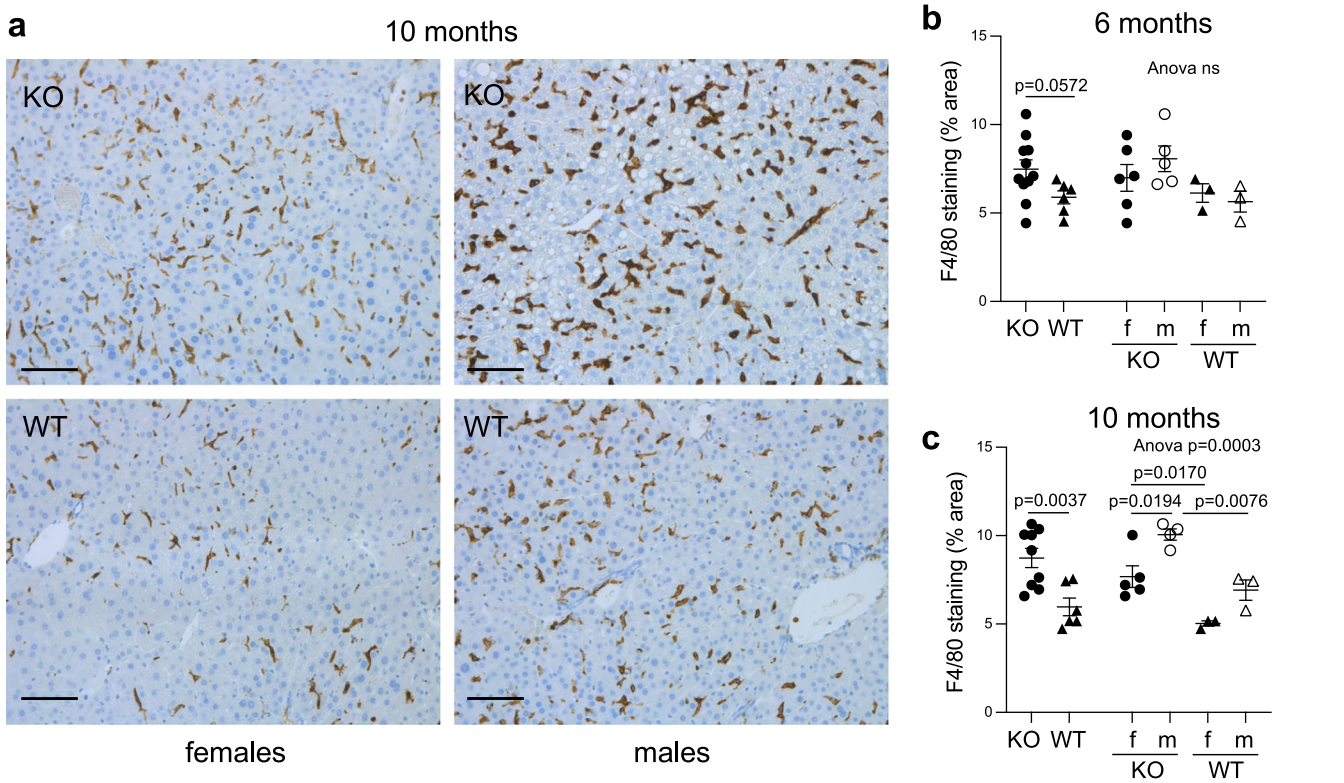

Fig. 5 | Staining for the F4/80 macrophage and Kupffer cells marker in the liver of cpKO and WT mice at 6 and 10 months of age. a representative images of the F4/80 staining (brown) for macrophage and Kupffer cells in the liver sections of 10 months-old mice; cell nuclei are evidenced by blue hematoxylin staining. Scale bars = 100 µm. **b**, **c** Quantitation of the F4/80 staining performed using QuPath software in animals at 6 months of age (*cp*KO $N = 11$, 6 females, 5 males; WT $N = 6$, 3 females, 3 males) and 10 months of age (*cp*KO $N = 9$, 5 females, 4 males; WT $N = 6$, 3 females, 3 males), respectively. Data are measured as percentage of the image area positive for F4/80 staining and reported as mean ± SEM, each dot corresponds to one animal. Statistical p-values were evaluated by unpaired Student' t-test for the direct comparison of *cp*KO and WT, and by ANOVA followed by Tukey's post-test for comparison of males and females across the two group of mice.

inflammation. Immunochemical staining for F4/80 antigen, a macrophages and Kupffer cells marker (Fig. 5a), showed a near-significant trend ($p = 0.0572$) towards increased levels in 6 months-old *cp*KO mice compared to WT (Fig. 5b), consistent with the inflammation of liver tissue previously reported in *cp*KO mice at this age[17,25]. However, no differences between *cp*KO females and males were observed, suggesting that a similar early inflammation occur in both sexes at 6 months of age (Fig. 5b), which in turn did not explain the larger ^{64}Cu-CP uptake observed in the liver of *cp*KO male mice (Fig. 2a). In 10 months-old mice, *cp*KO showed a significantly higher F4/80 antigen signal than WT mice, which was independent of sex (Fig. 5a and c). Furthermore, *cp*KO males manifested significantly more pronounced macrophages infiltration and/or Kupffer cells enlargement than females (Fig. 5a, c), which also in this case did not correlate with the larger uptake of ^{64}Cu-CP observed in females at 10 months (Fig. 2b).

Sex effects on the efficacy of CP-replacement in CP-deficient mice

We previously reported the efficacy of CP ERT in ameliorating both systemic and neurological symptoms in *cp*KO mice[18,19], with the same CP we employed for the radiolabelling studies described here. The overall therapeutic effect was clearly depicted in the results of principal components analysis (PCA) which took into consideration 33 different parameters measured whose described the pathophysiological state of each mouse[18]. That analysis was performed considering males and females together, since the animals underwent to the same therapeutic protocol (intraperitoneal administration of plasma-purified CP at 5 µg/g every 5 days for 4 months, from 6 to 10 months age). Thus, in the light of the differences between males and females in the [^{64}Cu]-CP uptake observed along age, we decided to assess sex-specific effects on the therapeutic efficacy in the published dataset.

As expected, the PCA performed on the same 33 measured parameters, showed a clear separation of the cluster of *cp*KO and WT mice in both sexes. While the efficacy of CP replacement therapy in both sexes was confirmed as demonstrated by separation of CP-treated *cp*KO animals from untreated *cp*KO mice, the separation CP-treated *cp*KO male mice from untreated male *cp*KO was complete and more pronounced to that observed in the corresponding female cohort, where CP-treated *cp*KO animals still presented a partial overlap with their untreated *cp*KO counterparts (Fig. 6). Therefore, we can conclude that the therapeutic effect in this animal model of ACP was more pronounced in males than females.

To evaluate whether the different therapeutic effect might depend on any sex-specific differences in pathological features during the disease progression of *cp*KO mice, we performed a re-analysis of our published data for untreated animals [data are available as Supplementary Data 5 in ref. 18]. We excluded from the analysis the features known to be sex-associated, like body and organs weight, and adipose tissue volume. The analysis was done for the animals at 6 and 10 months of age directly comparing the individual parameters and data are reported in Supplementary Table 1. We did not find significant sex-specific differences for the parameters associated to the neurodegeneration/neuroinflammation, both at 6 and 10 months of age, except for the iron deposition in the choroid plexus which was higher in males than females in older mice. Similarly, for liver damage-associated parameters, the sole difference was in the F4/80 antigen staining, which resulted to be higher in males than females at 10 months of age. The major differences between sexes were found in the hematological parameters associated to the erythropoiesis. Several of these parameters were significantly different between cpKO males and females at 6 months of age, with a worst pathological condition associated to the erythropoiesis in females than males. For example, circulating hemoglobin, hematocrit,

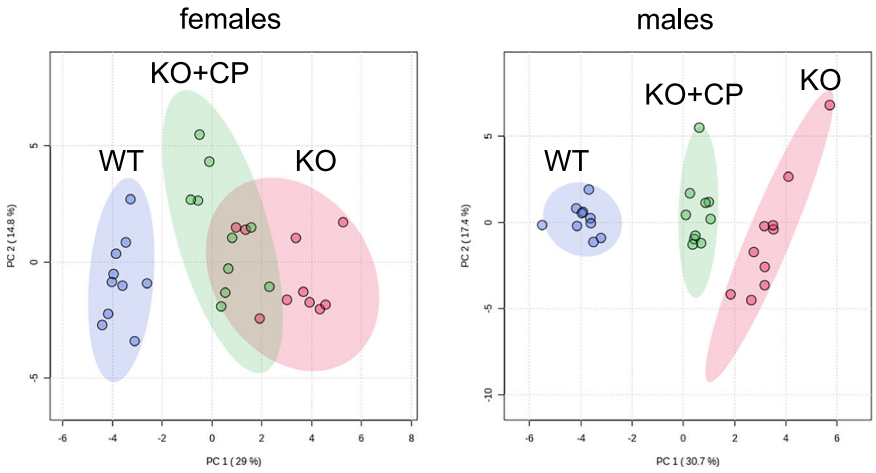

Fig. 6 | Unsupervised multivariate analysis of the overall therapeutic effect of the CP enzyme replacement therapy in males vs. females cpKO mice. Principal component analysis (PCA) of 33 parameters measured in WT and cpKO mice at 10 months of age and cpKO mice treated for 4 months with purified CP as reported in ref. 18. PCA was performed considering separately female and male animals ($N = 20$, 10 males and 10 females each group). Each dot represents one animal (CpKO = red; WT = blue; CpKO+Cp = green); ellipses represent the 95% confidence interval area of each group.

hemoglobin in reticulocytes and iron in serum were lower in females and vice versa the number and percentages of reticulocytes as well as platelets counts were higher in females than males. The difference between males and females cpKO mice in erythropoiesis-associated hematological parameters was maintained at 10 months only for few of the parameters, suggesting a worsening of the erythropoiesis symptoms in males during the disease progression. The re-analysis indicated that female cpKO mice showed a more pronounced dysregulation of erythropoiesis than males at the onset of the disease symptoms.

Discussion

Sex-specific differences in medicine represent an increasing focus of attention for personalized medicine. Identifying sex-specific differences in disease risk, penetrance, onset, phenotypes as well as in pharmacokinetics and susceptibility to adverse drug reactions is key to enable an accurate mechanistic understanding of disease and to demonstrate safety, tolerability and efficacy of candidate diagnostics and therapeutics in clinical trials. [reviewed in refs. 26–30]. In particular this is true for metabolic diseases where the differences between males and females are exacerbated[31]. Sex-associated differences in compound biodistribution have been investigated exploiting the use of radiolabelled compound and PET imaging analysis[23,32–34]. Our previously published demonstration of efficacy for CP ERT in cpKO mice did not take into account the possibility of sex-specific differences in the bioavailability of administered CP, which in turn may influence therapeutic efficacy in a sex-specific way[3,18,19]. In here, we address both aspects.

The major finding of this work is that the *cp*KO male mice display a higher uptake of administered CP than females in the early stage of the disease at 6 months of age, in particular in the liver and cerebellum (all brain in the ex vivo analysis). However, due to the proximity of the cerebellum and choroid plexus of the fourth ventricle, even in the lateral region of the cerebellum where the VOI was placed, we cannot rule out that part of the signal detected in the cerebellar region was due to ^{64}Cu-CP accumulation in the choroid plexus. Vice versa, at 10 months of age, when overt disease with neurodegeneration occurs, females showed a greater CP uptake than males. If considered longitudinally from 6 to 10 months of age, the opposite behavior of uptake between males and females seems to mainly depend on a dramatic increase of the uptake by females in all the organs during aging and to a lesser extent on reduction of the uptake in cerebellum and liver in males. Importantly, the observed sex- and age-dependent differences in bioavailability are genotype-dependent, as a different pattern is observed in *cp*KO and WT mice. Nevertheless, a possible limitation of our study is the low sample size that may have overlooked some other sex- or age-dependent differences.

The confirmation that the radioactive signal detected by PET/CT were a relevant proxy for the presence of the CP protein in the organs and not the measurements of free [^{64}Cu] released from the labeled protein, was inferred by the protein detection in the brain of the injected mice (Supplementary Fig. 2). Moreover, it has been reported that while the reversible dissociation of Cu from CP occurs in vitro, and is exploited for CP labeling, the exchange of the Cu incorporated in the CP with ionic Cu does not occur in vivo, where the Cu enters in the CP only during the synthesis of the protein and remains associated to it throughout its life span[35–37]. In the literature it has been reported that CP may be a source of copper for cells and that release of radiolabeled Cu from CP has been demonstrated to occur in vitro in cell culture via a regulated process on the cell membrane, which requires the close proximity/binding of CP with the membrane[36,37]. Therefore, we can't exclude that the signal from ^{64}Cu that we measured by PET and ex vivo might be from the intracellular ^{64}Cu internalized upon release from CP at the cell membrane level. Nevertheless, the close proximity/binding of CP with the cell membrane which is necessary for this mechanism in turn implies that the CP we injected in mice must have reached the target organs, therefore supporting the concept that our results reflect the biodistribution of the administered [^{64}Cu]-CP.

The differences in uptake between males and females in the time frame between 6 and 10 months of age are critical because represented the treatment time window used in our previous work for the ERT in this same preclinical model of ACP. Since ACP is an adult-onset disease, in humans this time window corresponds to the period of approximately 10 years that occurs between the appearance of systemic symptoms (diabetes, retinopathy, microcytic anemia) and the devastating neurological outcomes which rapidly evolve towards a poor prognosis[6,11,13,38]. In human, this period of time has been considered as a possible therapeutic window in which efficacious treatment could prevent the progression of the disease toward the neurodegeneration[6,38]. Based on the observed sex-specific, genotype-specific differences in CP bioavailability, we elected to assess the previously published, comprehensive analysis of therapeutic efficacy of CP ERT from the sex perspective, focusing on any differences in the response of male and female *cp*KO mice to CP ERT and on the influence which genotype may have on them. The unsupervised multivariated analysis indicated that, with the same protocol and dosage[18], the ERT resulted to be more efficacious in male than female *cp*KO mice although a therapeutic effect was observed in both sexes. Based on this evidence, we can hypothesize that the greater uptake in the liver and cerebellum at early time (6 months) for males seems to favor the rescue of the phenotype and is a favorable condition compared to having, after 4 months of treatment, a greater uptake in all organs as shown by females. In fact, the liver and the cerebellum are two of the target organs of the disease, therefore an early reconstitution of CP levels may prevent the accumulation of iron in the liver and the degeneration of Purkinje cells[3,18,19]. The reduced therapeutic effect shown in females could therefore be due to underdosing in the early phases of therapy as consequence of the lower uptake. Such sex-specific differences in the bioavailability of exogenously administered CP may not necessarily be translatable to ACP patients subjected to CP ERT, as we cannot exclude that it may

represent a species-specific effect. However, it may be important to consider this possibility in setting dosing regimens in ACP patients in future clinical trials, which could be tailored based on sex and age.

Why CP is differently accumulated in the organs of males and females is not known. We hypothesized that, at least for the liver, a more pronounced hepatic inflammation in males at 6 months of age, and for the females at 10 months age, might account for the larger [^{64}Cu]-CP uptake, merely depending on the inflammatory status of the organ (e.g. by increased vascular permeability or general metabolic demanding). However, this was not the case because both macrophages infiltration and Kupffer cells activation demonstrated a comparable sex-independent increase at 6 months of age in *cp*KO mice and were lower in female than male mice at 10-months of age. Thus, not reflecting the uptake of ^{64}Cu-CP observed, which was the opposite. Similar conclusions were inferred by the uptake of the [^{18}F]-VC701 tracer for TSPO, proxy of the inflammatory condition. Moreover, at 6 months of age the [^{64}Cu]-CP uptake was higher in the liver of males than females also in WT mice in the absence of signs of tissue inflammation. The WT mice also showed differences between males and females in [^{64}Cu]-CP uptake and accumulation in the cerebellum but with the opposite trend to that of *cp*KO mice at both 6 and 10 months of age. Furthermore, the generalized increase in [^{64}Cu]-CP accumulation in all organs observed in the *cp*KO females at 10 months of age was not evidenced in WT females. This indicated a specificity of the dynamics of CP accumulation in different organs associated with the genotype, and therefore with the pathological characteristics of ACP.

The different therapeutic efficacy of the ERT in *cp*KO mice, revealed by the re-analysis of our previously published results, might not depend on the different uptake of CP in males and females found in the present study. Indeed, the CP biodistribution after long-term treatment might be different from the biodistribution observed after single injection, even because they differed in the way of administration. The single injection was done intravenous while the long-term treatment was done by intraperitoneal administration, since intravenous was not practicable for repeated injections in mice. To face, partially this limitation, we re-analysed the data of CP detected by ELISA in the brain of cpKO mice long-term-treated with CP in our previous work[18], considering males versus females. The results showed that CP accumulation in the brain at the end of the long-term treatment occurred mainly in the female mice (Supplementary Fig. 4). This is analogous to the larger accumulation in females in the biodistribution analysis observed after a single injection in mice at 10 months of age, thus suggesting similar biodistribution both in long-term and single injection administration.

Differences in the therapeutic effect of the CP administration, could instead depend on a different onset and progression of the disease in males and females, which could favor or disfavor the uptake of the CP or its functionality. For example, it has been reported that CP circulating in the blood can functionally interact with several proteins (e.g. transferrin, lactoferrin, myeloperoxidase)[7,39]. The levels of these interactors in males and females of *cp*KO mice may vary and could affect the stability and or availability of the administered CP. We looked for sex-specific pathological features of *cp*KO mice at 6 and 10 months of age re-analysing the data from our previous work[18].

The major finding was a difference in the hematological parameters associated with erythropoiesis, mainly in 6 months old mice, where females showed more aggressive dysregulation than males. Whether and how this might directly explain the different CP uptake in young mice and the therapeutic effect observed in CP-treated animals at 10 months of age, deserves future investigations. Nevertheless, it is an interesting observation because some sex-associated differences regarding disease features and timing of ACP progression in humans have been revealed by recent meta-analysis of literature cases of ACP[40]. In particular, from the 110 ACP patients analysed, it results that in the first disease stage females are more likely to suffer from anaemia, like in the *cp*KO mice, while males are more subjected to diabetes[40]. Thus, the re-analysis further supports the translational value of the cpKO mouse as model for the human ACP. In humans, the extremely limited number of patients in the world and the great heterogeneity of symptoms and phenotypes in ACP do not allow for in-depth analysis of the sex-associated differences of the pathology. However, as ACP is a metabolic pathology, these differences can be expected. Additional studies are required to investigate other sex aspects related to the disease in both mice and humans and to the response to therapy, as well as to determine if gender effects uncovered in ACP mice are relevant to the human ACP context.

From this point of view, the vast majority of works done to characterize the preclinical model of ACP have been carried out exclusively on male CP-deficient animals, or the sex of the mice was not specified. To our best knowledge, in addition to our previously published works[3,17–19], only few other works[41,42] declared the use of both male and female animals in the studies. Furthermore, to our knowledge, in the literature (including our previous works) the results of the studies were not processed and interpreted considering the two sexes separately. This is a serious gap that will need to be filled in future studies for the characterization of the disease in preclinical models.

In conclusion, our work underlines the need to perform the study of ACP in the preclinical models considering the two sexes separately and point to the possibility of sex-specific therapeutic regimens in the design of future ceruloplasmin replacement therapies for this rare disease.

Methods

Animal model

Male and female *cp*KO mice (*mus musculus*) in the C57Bl/6 J genetic background were used[18,43], while, as control population, age- and sex-matched wild-type C57Bl/6 J mice (Charles River) were used. The study complied with all relevant ethical regulations and was approved by the Institutional Animal Care and Use Committee (IACUC ID 1256, IRCCS-San Raffaele Hospital) and by the National Ministry of Health (7/2022-PR).

Ceruloplasmin radiolabelling with ^{64}Cu. CP is a blue-copper enzyme containing 6 Cu atoms[1], thus, human CP purified from unused human plasma fractionation intermediate $FIV_{1\text{-}4}$[18] was radiolabelled with ^{64}Cu by isotope exchange as reported in ref. 35. Briefly, lyophilized CP (1 mg) was resuspended in ultra-pure water (1 mg/mL) and buffer replaced with sodium acetate 0.2 M, pH 5.6 using 50 kDa cut-off Amicon Ultra-0.5 Centrifugal Filter Unit (UCF 505096, Merck). After five buffer exchange rounds, the CP protein (132 KDa) concentrated in the filter was resuspended in 1 mL of acetate buffer. Then, 200 µg of CP in acetate buffer were labeled with 370 MBq $^{64}CuCl_2$ (Acom), adding 60 µl of ascorbic acid (2 mg/mL in sodium acetate buffer) as stabilizer agent, under helium flux by spontaneous isotope exchange, incubating the mixture for 90 min at 20 °C. To stop the labeling and to bind free radioactive copper present in the reaction solution, the chelating agent diethylenetriaminepentaacetic acid (DTPA) was added and then the quality of the labeled material was checked by high-performance liquid chromatography (HPLC) and radio-thin layer chromatography (TLC). Five µl of sample were seeded onto TLC plates (Agilent) run in 150 mM NaCl solution. HPLC was run in a XBridge Protein BEH SEC (Waters) size exclusion chromatography column using a mobile phase 100 mM phosphate buffer pH 6.8 at 0.86 mL/min flux. The yield of the radiochemical reaction was about 20% (not decay corrected), corresponding to about 74 MBq of ^{64}Cu bound to CP. Free copper was removed from radiolabelled CP by using 50 kDa cut-off Amicon Ultra-0.5 Centrifugal Filter Unit (Merck), the buffer was exchanged 3 time with PBS and ascorbic acid (15 min, 14,000 *g* at 4 °C) with the protein at final concentration of 1 mg/ml. The radiochemical purity of ^{64}Cu-CP was greater than 97% as evaluated by HPLC or equal to 100% as assessed by radio-TLC, indicating that the labeling process did not promote protein degradation (Supplementary Fig. 5).

In vivo and ex vivo analysis of ^{64}Cu-labeled CP accumulation/biodistribution in *cp*KO and WT mice

In vivo PET/CT kinetic studies were performed in the 6 months old *cp*KO mice ($N = 6$, 3 females and 3 males). The day of the experiment, animals were injected in the caudal vein with 5.12 ± 0.25 MBq of [^{64}Cu]-CP which corresponded to about 14 µg of CP and was on average 12.5 folds lower than the amount intraperitoneally administered to the mice in our previous works[18,19]. Mice were then scanned at different time points after injection: 1, 3 and 21 h. At each scan, animals were anaesthetised by isoflurane in medical air (2:1)

and positioned prone on the CT bed scanner (X-Cube, Molecubes, Gent) for a 2 min acquisition. After that, the bed with the immobilized animals was moved to the PET scanner (β-Cube, Molecubes, Gent) for a 30 min acquisition. Imaging data deriving from PET and CT were reconstructed, automatically co-registered and corrected for radioisotope decay. Data from each time point were then analysed using PMOD software (v4.0, PMOD Technologies, CH) and Volumes of Interest (VOIs) method. Circular VOIs were placed on trans-axial slices within the brainstem, cerebellum, heart wall, liver, femoral bone and chest muscle to obtain radioactivity concentration expressed as Standardized Uptake Value (SUV_{mean}).

Based on the results obtained from kinetics, 21 h was selected as the best time point to monitor [^{64}Cu]-CP accumulation in the brain and periphery of *cp*KO mice. In order to increase sample size and to compare accumulation in 6- and 10-month-old *cp*KO mice and in WT animals, an additional group of mice of 6 months of age has been added ($N = 6$ WT mice, 3 females and 3 males; and $N = 5$ *cp*KO mice, 3 females and 2 males). One *cp*KO male mouse was excluded from the analysis because of an error in the intravenous injection of the radioligand. Therefore, $N = 6$ WT (3 females and 3 males) and $N = 10$ *cp*KO mice (6 females and 4 males) of 6 months of age were analyzed in total. Then, a group of 10 months of age animals was evaluated: $N = 6$ WT mice (3 females and 3 males) and $N = 9$ *cp*KO mice (5 females and 4 males). Procedures for in vivo PET-CT acquisition were the same described in the previous section. At the end of the last PET acquisition, all animals were sacrificed by cardiac puncture to collect and organs (brain, eyes, liver, small intestine, lung, kidney, heart and chest muscle), for ex vivo biodistribution and immunohistochemical analysis. Radioactivity in whole organs was evaluated using gamma-counter (LKB Compugamma CS1282, Wallac). The data were expressed as SUV (Standardized Uptake Value), i.e., the radioactivity measured in the tissue divided by the radioactivity in the injected dose and all multiplied for the weight of the animal. Data were also expressed as tissue to muscle ratio to normalize retention in a specific tissue compared to background.

[^{18}F]-VC701 radiosynthesis

The automated synthesizer TRACERLAB FXFN (GE Healthcare, Milan, Italy) was used to prepare [^{18}F]-VC701. [^{18}F]F− was produced with the ^{18}O(p,n)^{18}F nuclear reaction by irradiation of [^{18}O]water. After anhydrification, the labeling was performed with the precursor VC622 (3 mg) in anhydrous DMSO at 140 °C for 20 min. The reaction mixture was purified by HPLC and the fraction corresponding to ^{18}F-VC701 was collected in sterile water followed by solid-phase extraction on pre-activated Sep-Pak tC-18 cartridge (Waters). [^{18}F]-VC701 was eluted with 0.7 mL ethanol and diluted with saline solution to 10 mL for the final formulation. Radiochemical purity of [^{18}F]-VC701 was higher than 99%.

In vivo and ex vivo analysis of accumulation/biodistribution of the translocator protein (TSPO) specific marker [^{18}F]VC701 in *cp*KO and WT mice

In vivo PET/CT study was performed in satellite groups of 10 months old *cp*KO mice ($N = 9$, 5 females and 4 males) and WT mice ($N = 9$, 6 females and 3 males). The day of the experiments, animals were injected in the caudal vein with 1.91 ± 0.27 MBq of [^{18}F]-VC701 and acquired at 2 h from the injection. The acquisition was performed as described above for [^{64}Cu]-CP: animals were anaesthetized with isoflurane in medical air (2:1) and subjected to 2 min acquisition with CT and 20 min acquisition with PET just after. At the end of acquisition, animals were sacrificed by cardiac puncture for the sampling of organs (brain, eyes, liver, small intestine, lung, kidney, heart and chest muscle) for gamma-counting. PET and gamma-counter data were analyzed as described above.

CP evaluation by ELISA

The level of human CP was evaluated by ELISA (Human Ceruloplasmin ELISA Kit, NBP2-60616 Novus Biologicals) in 300 µg of brain protein extracts obtained from the organs collected for the ex vivo analysis. Absorbance was measured at 450 nm with microplate reader (iMark, BioRad).

Immunohistochemistry analysis for liver macrophages infiltration and Kupffer cells enlargement

The analysis was performed on the liver of WT and *cp*KO mice of 6 and 10 months of age at the end of the biodistribution analysis. Liver specimens were fixed in 4% paraformaldehyde (16 h at 4 °C), transferred in 70% ethanol solution and embedded in paraffin. Automated immunostaining for F4/80 antigen, a marker for macrophage and Kupffer cells was performed with F4/80 (D2S9R) XP® Rabbit monoclonal antibody (CST#70076, Cell Signaling Technology) used at 1:200 dilution, followed by Leica Bond Polymer Refine Detection antibody (Leica, DS9800) ready to use reagent for automated detection in the Leica BOND RX instrumentation. The 3 µm thick sections were then counterstained with hematoxylin using the Leica BOND RX instrumentation at the Animal Histopathology facility, OSR. Samples were analysed with Zeiss AxioImager microscope. F4/80 positive areas on liver were quantified using QuPath software (https://github.com/qupath)[44] on average 2-3 images from two different tissue sections were acquired and quantified for each mouse.

Statistics and reproducibility

Data from two different groups were evaluated by unpaired Student's t-test, after checking the normality test for Gaussian distribution (Kolmogorov-Smirnov test or Shapiro Wilk test) of by Mann–Whitney test if they did not pass the test for normal distribution. Statistical significance among three or more groups was evaluated by one-way analysis of variance (ANOVA) and ad hoc post-test analysis to compare all pairs of groups (Tukey's test) if data pass the test for Gaussian distribution, or by Kruskal-Wallis test followed by Dunn's test post-hoc analysis if they didn't. In all analyses, performed with Prism V10.0 software (GraphPad Inc.), a two-tailed $p < 0.05$ was considered significant comparing means ± standard error (SEM). The sample size ($N = 6$) was established using the G-Power v3.1.9.4 software (Heinrich-Heine-Universität Düsseldorf), applying a unpaired student-t test or one-way ANOVA test for the comparison of means between 2 or 4 groups with alpha error of 0.05 and power of 0.8; effect size (Cohen's effect size) of 2. No acquired data where excluded from the analysis, with the exception of one mouse not included in the analysis because wrongly injected. Whenever possible 2-3 technical replicates for data acquisition were measured for each of the mice used as biological replicates. Data acquisition and analysis were performed in blind.

Multidimensional reduction analysis by unsupervised principal component analysis (PCA) was used for data mining analysis on the efficacy of ERT according to animal sex. We analysed together the 33 features collected in our previous study aimed to evaluate the efficacy of the CP replacement therapy in the CP-deficient mouse model [data are available as Supplementary Data 5 in ref. 18]. These parameters describe the pathophysiological state of each mouse. Data were from three groups of animals: WT and *cp*KO mice treated for 4 months with saline solution as control and *cp*KO mice treated with purified CP[18]. Parameters were collected at the end of the treatment when mice were 10 months old. Since the features were measured according to different scales, the data were normalized by auto-scaling transformation (mean-centered and divided by the standard deviation of each variable), and the analysis was performed using MetaboAnalyst 6.0 online package (www.metaboanalyst.ca/home.xhtml) considering males and females in separated groups. Upon PCA, the 2 principal components were reported and the experimental groups of animals were highlighted as 95% confidence interval area automatedly defined by the software.

Reporting summary

Further information on research design is available in the Nature Portfolio Reporting Summary linked to this article.

Data availability

The datasets of the current study are available at "San Raffaele Open Research Data Repository" (ORDR) (https://ordr.hsr.it/research-data/); https://doi.org/10.17632/5r9kkgbwhw.1. All the numerical source data of the graphs are available in the Supplementary Data Excel file.

Received: 23 August 2024; Accepted: 10 February 2025;
Published online: 19 February 2025

References

1. Hellman, N. E. & Gitlin, J. D. Ceruloplasmin metabolism and function. *Annu. Rev. Nutr.* **22**, 439–458 (2002).
2. Arner, E. et al. Ceruloplasmin is a novel adipokine which is overexpressed in adipose tissue of obese subjects and in obesity-associated cancer cells. *PLoS ONE***9**, e80274 (2014).
3. Raia, S. et al. Ceruloplasmin-deficient mice show dysregulation of lipid metabolism in liver and adipose tissue reduced by a protein replacement. *Int. J. Mol. Sci.* **24**, 1150 (2023).
4. Rouault, T. A., Zhang, D. L. & Jeong, S. Y. Brain iron homeostasis, the choroid plexus, and localization of iron transport proteins. *Metab. Brain Dis.* **24**, 673–684 (2009).
5. Klomp, L. W., Farhangrazi, Z. S., Dugan, L. L. & Gitlin, J. D. Ceruloplasmin gene expression in the murine central nervous system. *J. Clin. Investig.* **98**, 207–215 (1996).
6. Piperno, A. & Alessio, M. Aceruloplasminemia: waiting for an efficient therapy. *Front. Neurosci.* **12**, 903 (2018).
7. Vasilyev, V. B. Looking for a partner: ceruloplasmin in protein-protein interactions. *Biometals* **32**, 195–210 (2019).
8. Kono, S. et al. Biological effects of mutant ceruloplasmin on hepcidin-mediated internalization of ferroportin. *Biochim. Biophys. Acta* **1802**, 968–975 (2010).
9. Jeong, S. Y. & David, S. Glycosylphosphatidylinositol-anchored ceruloplasmin is required for iron efflux from cells in the central nervous system. *J. Biol. Chem.* **278**, 27144–27148 (2003).
10. Olivieri, S. et al. Ceruloplasmin oxidation, a feature of Parkinson's Disease CSF, inhibits ferroxidase activity and promotes cellular iron retention. *J. Neurosci.* **31**, 18568–18577 (2011).
11. Miyajima, H. Aceruloplasminemia. in *GeneReviews(R)* (eds. Pagon, R. A. et al.) (Seattle, 1993).
12. Vroegindeweij, L. H. P., Boon, A. J. W., Wilson, J. H. P. & Langendonk, J. G. Effects of iron chelation therapy on the clinical course of aceruloplasminemia: an analysis of aggregated case reports. *Orphanet. J. Rare Dis.* **15**, 105 (2020).
13. Marchi, G., Busti, F., Lira Zidanes, A., Castagna, A. & Girelli, D. Aceruloplasminemia: a severe neurodegenerative disorder deserving an early diagnosis. *Front. Neurosci.* **13**, 325 (2019).
14. Pelucchi, S. et al. Phenotypic heterogeneity in seven Italian cases of aceruloplasminemia. *Parkinsonism Relat. Disord.* **51**, 36–42 (2018).
15. Ondrejkovičová, M. et al. New mutation of the ceruloplasmin gene in the case of a neurologically asymptomatic patient with microcytic anaemia, obesity and supposed Wilson's disease. *BMC Gastroenterol.* **20**, 95 (2020).
16. Zheng, J., Chen, M., Liu, G., Xu, E. & Chen, H. Ablation of hephaestin and ceruloplasmin results in iron accumulation in adipocytes and type 2 diabetes. *FEBS Lett.* **592**, 394–401 (2018).
17. Mannella, V. et al. Lipid dysmetabolism in ceruloplasmin-deficient mice revealed both in vivo and ex vivo by MRI, MRS and NMR analyses. *FEBS Open Biol.* **14**, 258–275 (2024).
18. Zanardi, A. et al. New orphan disease therapies from the proteome of industrial plasma processing waste- a treatment for aceruloplasminemia. *Commun. Biol.* **7**, 140 (2024).
19. Zanardi, A. et al. Ceruloplasmin replacement therapy ameliorates neurological symptoms in a preclinical model of aceruloplasminemia. *EMBO Mol. Med.* **10**, 91–106 (2018).
20. Tridimas, A. et al. Three-year follow up of using combination therapy with fresh-frozen plasma and iron chelation in a patient with acaeruloplasminemia. *JIMD Rep.* **57**, 23–28 (2021).
21. Dusek, P., Schneider, S. A. & Aaseth, J. Iron chelation in the treatment of neurodegenerative diseases. *J. Trace Elem. Med. Biol.* **38**, 81–92 (2016).
22. Kono, S. Aceruloplasminemia: an update. *Int. Rev. Neurobiol.* **110**, 125–151 (2013).
23. Belloli, S. et al. 18F-VC701-PET and MRI in the in vivo neuroinflammation assessment of a mouse model of multiple sclerosis. *J. Neuroinflamm.* **15**, 33 (2018).
24. Di Grigoli, G. et al. Radiosynthesis and preliminary biological evaluation of [18F]VC701, a radioligand for translocator protein. *Mol. Imaging* **14**, 7290.2015.00007 (2015).
25. Chen, M. et al. Ceruloplasmin and hephaestin jointly protect the exocrine pancreas against oxidative damage by facilitating iron efflux. *Redox Biol.* **17**, 432–439 (2018).
26. Mauvais-Jarvis, F. et al. Sex and gender: modifiers of health, disease, and medicine. *Lancet* **396**, 565–582 (2020).
27. Soldin, O. P., Chung, S. H. & Mattison, D. R. Sex differences in drug disposition. *J. Biomed. Biotechnol.* **2011**, 1–14 (2011).
28. Della Torre, S. & Maggi, A. Sex differences: a resultant of an evolutionary pressure? *Cell Metab.* **25**, 499–505 (2017).
29. Baggio, G., Corsini, A., Floreani, A., Giannini, S. & Zagonel, V. Gender medicine: a task for the third millennium. *Clin. Chem. Lab. Med.* **51**, 713–727 (2013).
30. Allegra, S., Chiara, F. & De Francia, S. Gender medicine and pharmacology. *Biomedicines* **12**, 265 (2024).
31. Maggi, A. & Della Torre, S. Sex, metabolism and health. *Mol. Metab.* **15**, 3–7 (2018).
32. Clemente, G. S. et al. [18 F]Atorvastatin pharmacokinetics and biodistribution in healthy female and male rats. *Mol. Pharmaceutics* **18**, 3378–3386 (2021).
33. Murtaj, V. et al. Brain sex-dependent alterations after prolonged high fat diet exposure in mice. *Commun. Biol.* **5**, 1276 (2022).
34. Rischka, L. et al. Biodistribution and dosimetry of the GluN2B-specific NMDA receptor PET radioligand (R)-[11C]Me-NB1. *EJNMMI Res.* **12**, 53 (2022).
35. Sternlieb, I., Morell, A.G., Tucker, W.D., Greene, M.W. & Scheinberg, I.H. The incorporation of co into ceruloplasmin in vivo: studies with co and copper. 40, 1834–1840 (1961).
36. Ramos, D. et al. Mechanism of copper uptake from blood plasma ceruloplasmin by mammalian cells. *PLoS ONE***11**, e0149516 (2016).
37. Percival, S. S. & Harris, E. D. Copper transport from ceruloplasmin: characterization of the cellular uptake mechanism. *Am. J. Physiol.* **258**, C140–C146 (1990).
38. Vroegindeweij, L. H. et al. Aceruloplasminemia presents as Type 1 diabetes in non-obese adults: a detailed case series. *Diabet. Med.* **32**, 993–1000 (2015).
39. Chapman, A. L. P. et al. Ceruloplasmin is an endogenous inhibitor of myeloperoxidase. *J. Biol. Chem.* **288**, 6465–6477 (2013).
40. Ketata, I. & Ellouz, E. New view of aceruloplasminemia: Systematic review and meta-analysis tracking dots from onset to disease development and iron-related features. *Rare* **1**, 100010 (2023).
41. Shiva, S. et al. Ceruloplasmin is a NO oxidase and nitrite synthase that determines endocrine NO homeostasis. *Nat. Chem. Biol.* **2**, 486–493 (2006).
42. Gresle, M. M. et al. Ceruloplasmin gene-deficient mice with experimental autoimmune encephalomyelitis show attenuated early disease evolution. *J. Neurosci. Res.* **92**, 732–742 (2014).
43. Patel, B. N. et al. Ceruloplasmin regulates iron levels in the CNS and prevents free radical injury. *J. Neurosci.* **22**, 6578–6586 (2002).
44. Bankhead, P. et al. QuPath: Open source software for digital pathology image analysis. *Sci. Rep.* **7**, 16878 (2017).

Acknowledgements

We thank the Animal Histopathology and Biochemistry facilities at the IRCCS-Hospital San Raffaele for assistance. This work was supported by Ricerca Finalizzata 2018, Italian Ministry of Health (RF-2018-12366471). The Italian Ministry for University and Research (MIUR) is gratefully acknowledged for yearly FOE funding to the Euro-BioImaging Multi-Modal Molecular Imaging Italian Node (MMMI). We acknowledge financial support under the National Recovery and Resilience Plan (NRRP), Mission 4, Component 2,

Investment 3.1 by the Italian Ministry of University and Research (MUR), funded by the European Union – NextGenerationEU – Project IR0000023: "STRENGTHENING THE ITALIAN INFRASTRUCTURE OF EURO-BIOIMAGING (SEELIFE)", CUP B53C22001810006.

Author contributions

Conceptualization, M.A. Methodology A.Z., C.M., A.Col., S.B., P.R., R.M.M. and A.Ca. Investigation, A.Z., A.Con., C.M., A.Col., S.B., P.R. and R.M.M. A.ca. provided purified ceruloplasmin. Funding Acquisition, M.A and S.B. Supervision, M.A. and R.M.M. Writing – original draft, M.A. and S.B. Writing – review & editing, M.A., S.B. and A.Ca. All the authors discussed the results and commented on the manuscript at all stages.

Competing interests

The authors declare the following competing interests: A.Ca. is employee of Kedrion S.p.A. All other authors declare no competing interests.

Additional information

Supplementary information The online version contains supplementary material available at https://doi.org/10.1038/s42003-025-07714-8.

Correspondence and requests for materials should be addressed to Massimo Alessio.

Peer review information *Communications Biology* thanks Maria Carmela Bonaccorsi di Patti and the other, anonymous, reviewer(s) for their contribution to the peer review of this work. Primary Handling Editors: Ibrahim Javed and David Favero. A peer review file is available.